Journal of Applied Polymer Science

Synthesis and Photocatalytic Performance of PVA/TiO_2/Graphene-MWCNT Nanocomposites for Dye Removal

Gowun Jung, Hyung-Il Kim
Department of Fine Chemical Engineering and Applied Chemistry, Chungnam National University, Daejeon 305-764, Korea
Correspondence to: H.-I. Kim (E-mail: hikim@cnu.ac.kr)

ABSTRACT: TiO_2/graphene-MWCNT nanocomposite was prepared using solvothermal reaction for the effective distribution of TiO_2 nanoparticles on carbonaceous materials. TiO_2/graphene-MWCNT nanocomposite was immobilized in poly(vinyl alcohol) (PVA) matrix for a convenient recovery after wastewater purification. MWCNT was incorporated in a nanocomposite not only to prevent the restacking of graphene but also to increase the electron transfer from TiO_2. The detailed characterization of the nanocomposite was performed using SEM, EDX, XRD, XPS, and FTIR. The photocatalytic performance of PVA/TiO_2/graphene-MWCNT nanocomposite was investigated by UV spectroscopy on the basis of degradation of organic pollutants. PVA/TiO_2/graphene-MWCNT nanocomposite showed improved photocatalytic decomposition of more than 70% of residual dye left in case of using PVA/TiO_2/graphene nanocomposite due to the improved electron transfer and the higher adsorption of organic pollutants. PVA/TiO_2/graphene-MWCNT nanocomposite was suitable as a promising material for the recyclable photocatalytic wastewater purification system. © 2014 Wiley Periodicals, Inc. J. Appl. Polym. Sci. **2014**, *131*, 40715.

KEYWORDS: composites; nanotubes; graphene and fullerenes; hydrophilic polymers; properties and characterization

Received 21 November 2013; accepted 11 March 2014
DOI: 10.1002/app.40715

INTRODUCTION

Recently, the wastewater containing organic pollutants is regarded as one of major serious problems in various industries. A variety of organic molecules such as dyes, phenols, and nitroaromatics causes harmful effect on the water environment generally due to low degradation ability and toxicity.[1] The removal of these organic compounds from wastewater is required indeed since small amount of dye is clearly visible and affects water quality adversely.[2] Therefore, many researchers have attempted to develop an effective material in order to improve the water purification efficiency.

Photocatalytic system is known to be a desirable method for degradation of environmental pollutants among various methods for wastewater treatment. Titanium dioxide (TiO_2) is a suitable photocatalyst for degradation of environmental pollutants because of its outstanding photocatalytic performance.[3,4] However, the use of TiO_2 as photocatalyst has certain limitations due to the recombination of photo-holes and photo-electrons generated in the photocatalytic process.[5] The recycling of TiO_2 nanoparticles after the photocatalytic decomposition of organic pollutants is also a problem to be solved for a wide expansion of commercial application.

The carbonaceous materials showed generally good electrical conductivity, large surface area, and facilitated adsorption of chemicals, which contributed to an effective photodegradation of pollutants.[6] The carbonaceous materials work also as an electron sink for hindrance of charge carrier recombination. Graphene has unique electrical, mechanical, and thermal properties among various carbonaceous materials. Therefore, graphene is employed in many nanocomposite applications.[7–13] However, graphene tends to restack easily to return to a graphite structure resulting in the deterioration of performance efficiency. Multiwalled carbon nanotubes (MWCNTs) were employed together with graphene sheets to prevent the restacking of graphene as well as to improve the electron conduction further.[14–18]

Many researchers studied TiO_2 photocatalyst and tried to improve the photocatalytic efficiency. Poly(vinyl alcohol) (PVA)/TiO_2 was prepared for dye decomposition by electrospinning method.[19] TiO_2/graphene composite was obtained via hydrothermal reaction of graphene oxide (GO)/commercial P25 and was investigated for the degradation of rhodamine B.[20] However, both photocatalytic activity of TiO_2 and recycling of photocatalyst need to be improved further for the practical applications. In this study, we used TiO_2 as a photocatalyst and carbonaceous materials as additives to improve the photocatalytic activities

effectively. In order to disperse TiO_2 nanoparticles uniformly on graphene-MWCNT surface, TiO_2/graphene-MWCNT nanocomposite was synthesized by a solvothermal reaction. The combination of photocatalyst nanocomposite and a polymeric substrate is attractive in solving the problem of recovery of a photocatalyst. PVA is a hydrophilic polymer, which has been extensively explored as biomaterial, drug delivery systems, sensors, and surgical repairs because of its excellent mechanical properties, biocompatibility, and nontoxicity. Therefore, PVA was employed as a suitable polymeric substrate for the photocatalytic wastewater treatment. TiO_2/graphene-MWCNT nanocomposite was immobilized in a PVA substrate to form PVA/TiO_2/graphene-MWCNT nanocomposites for an easier recovery of photocatalyst system. The photocatalytic activity of nanocomposite was studied in the decomposition process of model pollutant dye under UV irradiation. The photocatalytic performance of PVA/TiO_2/graphene-MWCNT nanocomposite was investigated in terms of the decomposition of model pollutant dye depending on the component of photocatalyst system.

EXPERIMENTAL

Materials

PVA (M_w: 31,000–50,000 g/mol), titanium (IV) isopropoxide (TTIP) used in this study were obtained from Sigma Aldrich (USA). MWCNTs grown by chemical vapor deposition were supplied by Sigma Aldrich (USA). MWCNTs had an average diameter of 30–50 nm and a length of 1–2 μm. *m*-Chloroperoxy benzoic acid (MCPBA) used for the chemical modification of MWCNTs was obtained from Sigma Aldrich (USA). GO was prepared by Hummers method[21] using the graphite obtained from Samchun Chemical (Korea). Glutaraldehyde (GA) obtained from Acros Chemical Company was used as the crosslinking agent for PVA. Methylene blue (MB), a model pollutant dye, was obtained from Acros Organics (USA).

Preparation of Graphene/MWCNT Nanocomposite

MCPBA of 3 g was added in benzene of 100 mL followed by the addition of MWCNT of 0.1 g. Then, the mixture was kept at 60°C for 6 h in an air atmosphere. After completion of modification, the mixture was filtered and dried at 60°C to remove the solvent and to obtain the modified MWCNT (m-MWCNT). GO and m-MWCNT were added in ethanol followed by sonication at room temperature for 120 min. The well dispersed GO/m-MWCNT mixture was separated and treated thermally at 200°C for 24 h to convert GO/m-MWCNT mixture into graphene-MWCNT mixture.

Synthesis of TiO_2/Graphene-MWCNT Nanocomposite

TiO_2/graphene-MWCNT nanocomposite was synthesized by solvothermal reaction to form TiO_2 nanoparticles on the surface of carbon materials uniformly. About 20 mg of GO and 10 mg of m-MWCNTs were sonicated in 90 mL of ethanol for 120 min using an ultrasonicator to form a suspension. TTIP was added slowly into GO/m-MWCNT suspension followed by thermal treatment at 200°C for 24 h. The reduction of GO and m-MWCNT induced TTIP to be oxidized to TiO_2 resulting in a simultaneous deposition of TiO_2 nanoparticles on the surface of carbon materials during the solvothermal reaction.

Preparation of PVA/TiO_2/Graphene-MWCNT Nanocomposite

PVA/TiO_2/graphene-MWCNT nanocomposite was synthesized by crosslinking the mixture of PVA and TiO_2/graphene-MWCNT nanocomposite. The crosslinking was carried out using GA (0.5 wt % to PVA) as a crosslinker of PVA. PVA solution (10 wt % wt/vol) was prepared by dissolving PVA in deionized water for 6 h at 90°C and subsequent cooling to room temperature. TiO_2/graphene-MWCNT (3 wt %) suspension was prepared in 5 mL ethanol by sonication for 60 min. TiO_2/graphene-MWCNT suspension was added in a PVA solution with a constant stirring. The mixture of PVA and TiO_2/graphene-MWCNT was stirred for 30 min at room temperature followed by nitrogen bubbling through the mixture for 20 min to remove the oxygen dissolved in the mixture. GA of 1 mL was added in PVA/TiO_2/graphene-MWCNT mixture followed by stirring for 6 h at room temperature for the crosslinking reaction. After addition of hydrochloric acid (35%) of 0.5 mL in the mixture, the crosslinking reaction was completed after 10 min at room temperature. PVA/TiO_2/graphene-MWCNT nanocomposite was washed with distilled water at room temperature by replacing with fresh distilled water every few hours to remove non-reacted materials. PVA/TiO_2/graphene-MWCNT nanocomposite was cut into a cubic shape of about 2 cm^3. The nanocomposite was dried at 60°C for 24 h in vacuum.

Characterization of TiO_2/Graphene-MWCNT Nanocomposite

Fourier-transform infrared spectrometer (FTIR, FTS-175C, Cambridge, USA) was used to investigate the functional groups of nanocomposite. FTIR spectra of samples were obtained in the range of 500–4000 cm^{-1}.

X-ray photoelectron spectroscopy (XPS) spectra were obtained using a MultiLab 2000 spectrometer (Thermo Electron Corporation, UK) to investigate the elements present in TiO_2/graphene-MWCNT nanocomposite. Al Kα (1485.6 eV) was used as X-ray source with a 14.9 keV anode voltage, a 4.6 Å filament current, and a 20 mA emission current. All samples were treated at 10^{-9} mbar to remove impurities. The survey spectra were obtained at 50 eV pass energy and at 0.5 eV step size.

The structures of graphene-MWCNT and TiO_2/graphene-MWCNT nanocomposites were studied using X-ray diffraction (XRD) patterns. The samples were investigated on a D8 Advance (Bruker AXS, Germany) diffractometer with Cu radiation and were analyzed from 20° to 80° in 2θ with a step size of 0.02° and a step time of 3 s.

Morphologies of PVA/TiO_2/Graphene-MWCNT Nanocomposite

The surface morphology of TiO_2/graphene-MWCNT and the cross-sectional morphology of PVA/TiO_2/grapene-MWCNT nanocomposite were investigated using a field emission scanning electron microscope (FE-SEM, S-5500, Hitachi, Japan) and its energy dispersive X-ray (EDX) spectrum were obtained. Every sample was sputter coated with Pt as a pretreatment. FE-SEM images were obtained at 10 kV.

Dye adsorption Behavior of PVA/TiO_2/Graphene-MWCNT Nanocomposites

The dye adsorption tests were carried out using 50 mL of MB solution with an initial concentration of 10 mg/L for PVA/TiO_2/

graphene-MWCNT nanocomposites. The nanocomposites were placed in a dye solution at 25°C in dark, respectively. The variations in concentration of dye solution were measured by UV spectrometer (Optizen 2120 UV, Mecasys, Korea) at a wavelength of 665 nm corresponding to the maximum absorption position of MB. The adsorption (Q) was calculated as follows.

$$Q\ (\mathrm{mg/g}) = (C_0 - C_t)V/W$$

where C_0 (mg/L) is the initial dye concentration, C_t (mg/L) is the dye concentration at time t, V (L) is the volume of dye solution, and W (g) is the weight of PVA/TiO_2/graphene-MWCNT nanocomposite.

Photocatalytic Activity of PVA/TiO_2/Graphene-MWCNT Nanocomposites

The photocatalytic degradation of MB was investigated in order to evaluate the photocatalytic activity of PVA/TiO_2/graphene-MWCNT nanocomposites. The dye decomposition experiments were carried out in a 150-mL cylindrical glass reactor equipped with an ultraviolet (UV) lamp (365 nm, 800 W) inside using a dye solution with an initial concentration of 10 mg/L. The variations in concentration of model pollutant dye were determined by UV spectrometer (Optizen 2120 UV, Mecasys, Korea) based on the absorbance at the wavelength of 665 nm for MB. The concentration of MB in a test solution was determined as a function of photodegradation activity. The cyclic dye decomposition experiments are also carried out to investigate both long-term stability and photocatalytic reproducibility of PVA/TiO_2/graphene-MWCNT nanocomposite under UV light irradiation. The photocatalytic dye decomposition efficiency (De%) was calculated by the following equation.

$$De\% = (C/C_0) \times 100$$

where C_0 and C are the concentrations of dye solution at $t = 0$ and t, respectively.

RESULTS AND DISCUSSION

Characterization of Graphene-MWCNT and TiO_2/Graphene-MWCNT Nanocomposites

FTIR spectroscopy was used to confirm the structures of both graphene-MWCNT and TiO_2/graphene-MWCNT nanocomposites. FTIR spectra of both samples are shown in Figure 1. Although graphene-MWCNT did not show any noticeable characteristic peaks, TiO_2/graphene-MWCNT showed several new peaks such as Ti—O and Ti—O—Ti stretching vibration at 500–1000 cm^{-1} and Ti—O—C vibration at 1400–1600 cm^{-1}. Moreover, the broad peak in the range of 3000–3500 cm^{-1} was attributed to O—H stretching vibration of Ti—OH group and water. The existence of Ti—O—C group indicated especially that the interaction between Ti and C was effectively produced during the solvothermal reaction.

The functional groups of graphene-MWCNT and TiO_2/graphene-MWCNT nanocomposites were evaluated by XPS analysis as shown in Figure 2. Both samples had C1s peak at 284.1 eV and O1s peak at 532.6 eV due to the partial oxidation of graphene and MWCNT. C1s deconvolution data of graphene-MWCNT and TiO_2/graphene-MWCNT nanocomposites are also

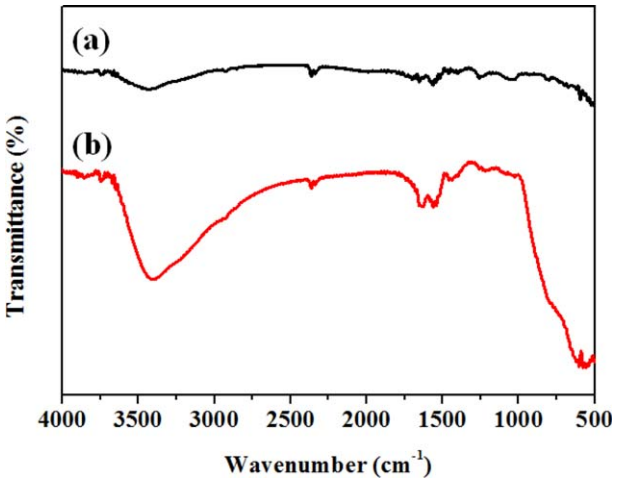

Figure 1. FTIR spectra of (a) graphene-MWCNT and (b) TiO_2/graphene-MWCNT. [Color figure can be viewed in the online issue, which is available at wileyonlinelibrary.com.]

shown in Figure 2(c,d). The peaks observed at 284.3, 285, 286.5, and 288.5 eV were assigned to C—C, C—H, C—OH, and C—O—Ti groups, respectively.[22–24] Figure 2(e,f) displayed the XPS spectra of Ti2p for graphene-MWCNT and TiO_2/graphene-MWCNT nanocomposites. $Ti2p_{3/2}$ and $Ti2p_{1/2}$ spin orbital splitting photoelectrons were located at the binding energies of 458.75 and 465 eV, respectively.[25] Compared to graphene-MWCNT nanocomposite, TiO_2/graphene-MWCNT showed slightly lower O1s peak intensity and had various Ti-related peaks. The reduction of carbon materials was believed to be accompanied with a simultaneous deposition of TiO_2 nanoparticles on the surface of carbon materials during the solvothermal reaction on the basis of XPS results.

The crystalline structures of graphene-MWCNT and TiO_2/graphene-MWCNT nanocomposites were studied by XRD. As shown in Figure 3, graphene-MWCNT had different peaks at 25.5°(002), 26.6°(002), and 42.5°(100), respectively. On the other hand, TiO_2/grpahene-MWCNT exhibited diffraction peaks at 25.3°(101), 37.5°(004), 47.6°(200), 54.2°(105), and 55.1°(211), respectively. These peaks indicated that anatase TiO_2 was effectively formed during the solvothermal reaction in the preparation of TiO_2/graphene-MWCNT nanocomposite. However, TiO_2/graphene-MWCNT nanocomposite showed only the low intensities of original TiO_2 crystalline diffraction peaks due to the interaction between TiO_2 and carbon materials.

Morphology Analysis of PVA/TiO_2/Graphene-MWCNT Nanocomposite

The surface morphologies of TiO_2/graphene-MWCNT and PVA/TiO_2/graphene-MWCNT nanocomposites were investigated by FE-SEM as shown in Figure 4. TiO_2 nanoparticles were homogeneously dispersed on the carbon materials as seen in Figure 4(a). TiO_2/graphene-MWCNT particles were also observed in the PVA matrix without any noticeable deformation or crack as shown in Figure 4(b). The high conductivity of carbon materials was effective in hindering the recombination of electrons and holes generated from TiO_2 due to the homogeneous dispersion of TiO_2 nanoparticles on the carbon materials.[26,27] As a

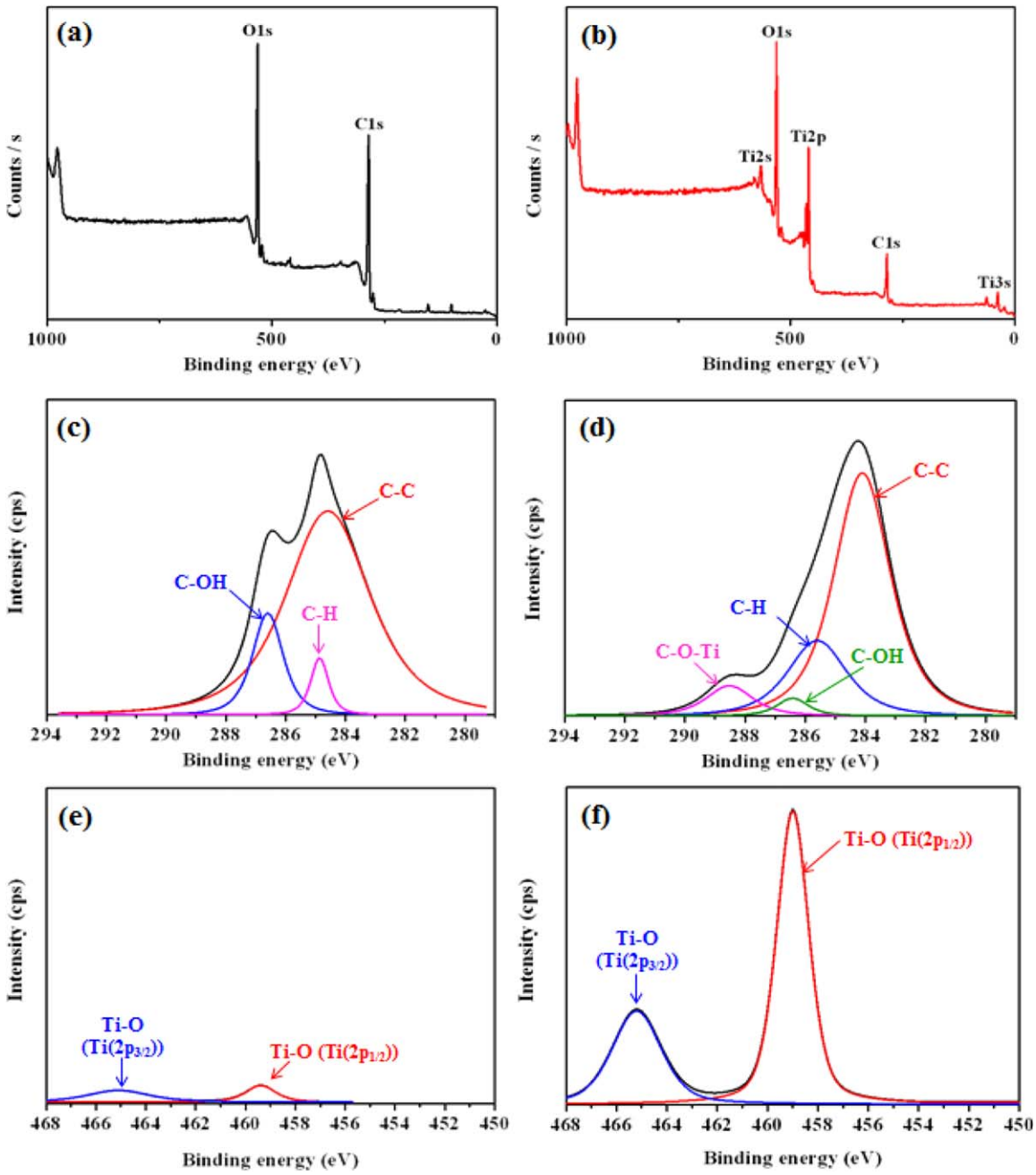

Figure 2. XPS results of graphene-MWCNT and TiO_2/graphene-MWCNT; (a) XPS elemental survey data of graphene-MWCNT, (b) XPS elemental survey data of TiO_2/graphene-MWCNT, (c) C1s deconvolution of graphene-MWCNT, (d) C1s deconvolution of TiO_2/graphene-MWCNT, (e) Ti2p deconvolution of graphene-MWCNT, and (f) Ti2p deconvolution of TiO_2/graphene-MWCNT. [Color figure can be viewed in the online issue, which is available at wileyonlinelibrary.com.]

result, PVA/TiO_2/graphene-MWCNT nanocomposite had an advantageous morphology to give improved photocatalytic efficiency due to an intimate contact between TiO_2 photocatalyst and carbon conductors and to give an easier recycling of photocatalyst after photocatalytic treatment due to a tight immobilization of TiO_2/graphene-MWCNT in PVA matrix. EDX spectrum of PVA/TiO_2/graphene-MWCNT demonstrated the distribution of Ti, C, and O components confirming the immobilization and the exposure of TiO_2/graphene-MWCNT in PVA matrix as shown in Figure 4(c). These morphological characteristics were beneficial for the enhanced photocatalytic efficiency because TiO_2/graphene-MWCNT photocatalyst nanocomposite dispersed in PVA matrix was able to be irradiated readily with UV.

Dye Adsorption Behavior of PVA/TiO_2/Graphene-MWCNT Nanocomposite

MB adsorption test was carried out to examine the adsorption characteristics of PVA/TiO_2/graphene-MWCNT nanocomposite depending on time. PVA/graphene-MWCNT nanocomposite

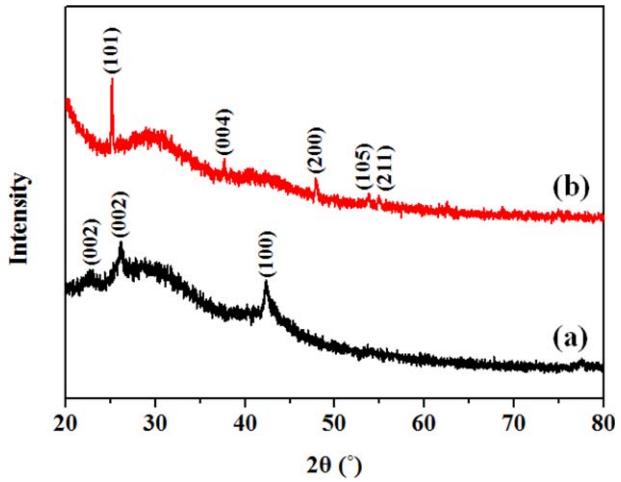

Figure 3. XRD spectra of (a) graphene-MWCNT and (b) TiO_2/graphene-MWCNT. [Color figure can be viewed in the online issue, which is available at wileyonlinelibrary.com.]

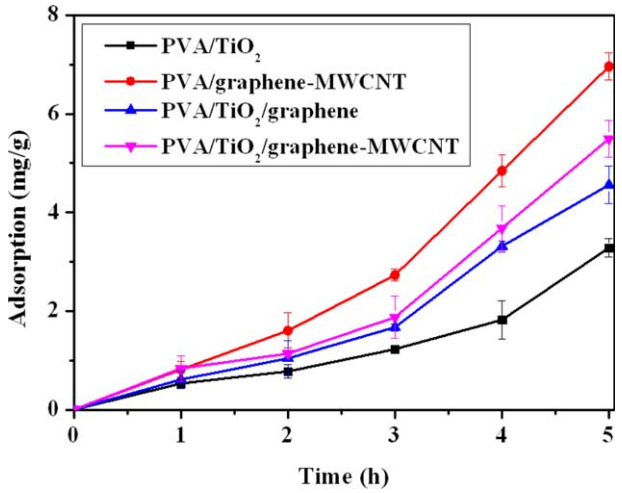

Figure 5. Dye adsorption capacities of various nanocomposite samples. [Color figure can be viewed in the online issue, which is available at wileyonlinelibrary.com.]

showed the highest dye adsorption capacity due to the contribution of carbon materials with larger surface area as seen in Figure 5. However, the existence of TiO_2 nanoparticles led to a certain decrease in adsorption capacities. It was attributed that TiO_2 nanoparticles were primarily placed on the surface of carbon materials resulting in partial blocking of pores of carbon materials. Compared to PVA/TiO_2/graphene nanocomposite, PVA/TiO_2/graphene-MWCNT nanocomposite showed better adsorption performance since MWCNT played an important role in supplying the available adsorption sites in carbon materials due to the effective prevention of graphene restacking. The adsorption characteristics of nanocomposites also had a close relation with the photocatalytic decomposition of pollutant dye solution.

Photocatalytic Dye Decomposition Behavior of PVA/TiO_2/Graphene-MWCNT Nanocomposite

The dye decomposition of all the nanocomposites was evaluated by the degradation of MB solution under UV light irradiation as shown in Figure 6. PVA/TiO_2/graphene-MWCNT nanocomposite showed the best decomposition efficiency for the degradation of MB. PVA/graphene-MWCNT, which did not contain

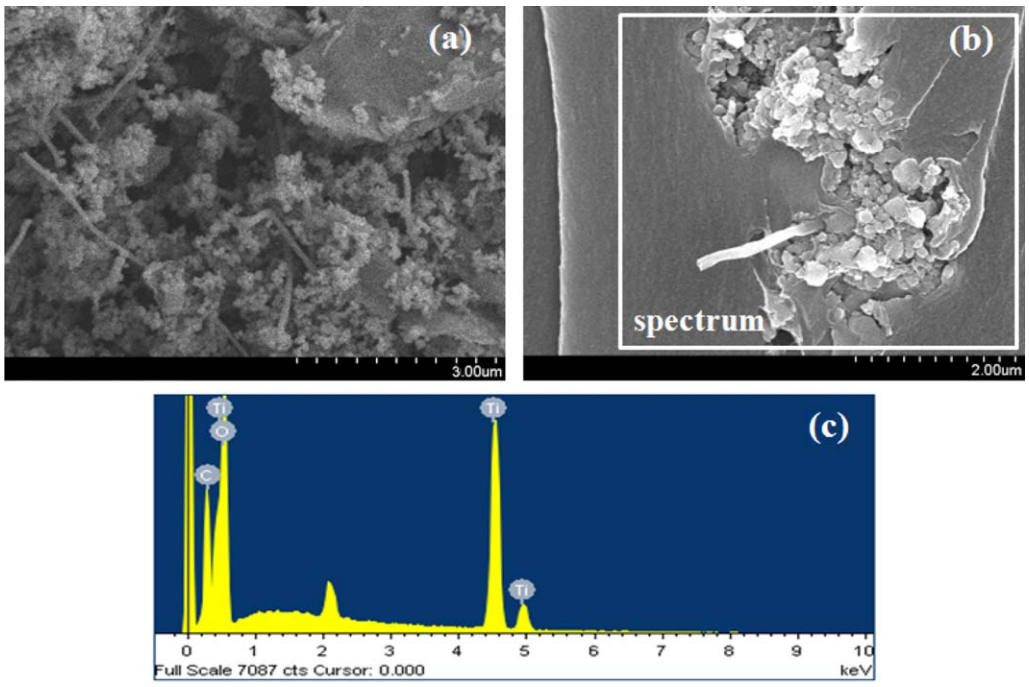

Figure 4. SEM images of (a) TiO_2/graphene-MWCNT nanocomposite, (b) PVA/TiO_2/graphene-MWCNT nanocomposite, and (c) EDX spectrum of PVA/TiO_2/graphene-MWCNT nanocomposite. [Color figure can be viewed in the online issue, which is available at wileyonlinelibrary.com.]

the photocatalyst TiO_2, showed the limited apparent removal of pollutant dye mainly by simple adsorption on carbon materials or penetration into PVA matrix. However, TiO_2-containing nanocomposites showed the considerable improvement in a photocatalytic decomposition of MB solution together with carbon materials. It was attributed to the effective prevention of electron–hole recombination in TiO_2 photocatalyst under UV irradiation by the coexistence of conductive carbon materials.[26,27] PVA/TiO_2/graphene-MWCNT nanocomposite showed even better photocatalytic activity in MB decomposition in comparison to PVA/TiO_2/graphene nanocomposite since the addition of MWCNT hindered the restacking of graphene in some part to give more space in carbon materials for deposition of TiO_2 nanoparticles. As a result, the photo-generated electrons from UV-irradiated TiO_2 nanoparticles were effectively transferred to the carbon materials resulting in the prevention of the recombination of holes and electrons from TiO_2 and improved the photocatalytic activity of nanocomposites.

Recycling and Long-Term Stability of PVA/TiO_2/Graphene-MWCNT Nanocomposite

The recycling tests were carried out using PVA/TiO_2/graphene-MWCNT nanocomposite in MB solution of pH 7 in order to confirm the long-term stability of photocatalytic behavior. PVA/TiO_2/graphene-MWCNT nanocomposite was placed in the pH 7 buffer solution to remove any residual pollutant dye followed by vacuum drying at 60°C for 24 h after every photocatalytic decomposition test. The cleaned PVA/TiO_2/graphene-MWCNT nanocomposite was used consecutively for the next cycle of photocatalytic decomposition test. As shown in Figure 7, the photocatalytic activity of PVA/TiO_2/graphene-MWCNT nanocomposite was maintained more than 90% after three consecutive cycles although some limited deterioration of photocatalytic activity was inevitable in each recycling step. Although the photocatalytic decomposition efficiency was somewhat decreased after repeated usage, PVA/TiO_2/graphene-MWCNT nanocomposite seemed to be eligible as a potential recyclable photocatalyst system for a wastewater treatment.

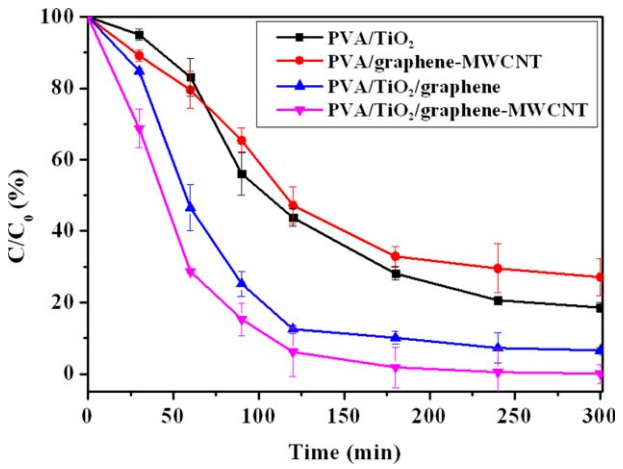

Figure 6. Photocatalytic dye decomposition behavior of various nanocomposite samples. [Color figure can be viewed in the online issue, which is available at wileyonlinelibrary.com.]

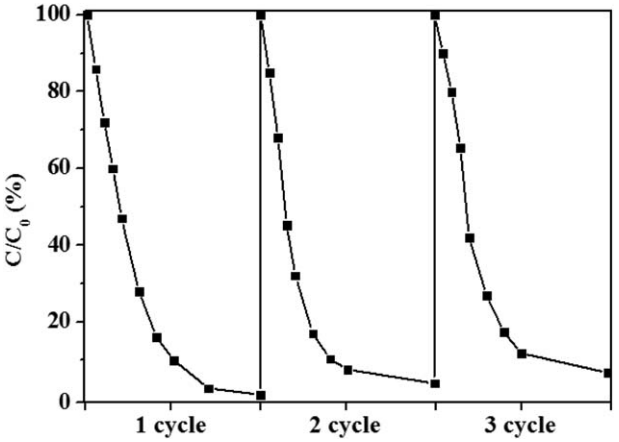

Figure 7. Cyclic photocatalytic pollutant decomposition behavior of PVA/TiO_2/graphene-MWCNT nanocomposite.

CONCLUSIONS

TiO_2/graphene-MWCNT nanocomposite was successfully prepared by a solvothermal reaction and PVA/TiO_2/graphene-MWCNT nanocomposite was prepared by crosslinking the mixture of PVA and photocatalyst nanocomposite. TiO_2 nanoparticles were homogeneously formed on the carbon materials using the solvothermal reaction. The photocatalytic activity of TiO_2 for the pollutant decomposition was improved significantly by combining graphene and MWCNT with TiO_2. MWCNT played an important role in preventing the restacking of conductive graphene. Both graphene and MWCNT contributed a lot in the improvement of photocatalytic activity of TiO_2 by both accelerating the interfacial electron transfer between UV-irradiated TiO_2 and carbon materials and adsorbing the pollutants effectively on the available adsorption sites of carbon materials.

ACKNOWLEDGMENTS

This work was supported by National Research Foundation of Korea (Project 2012R1A1A4A01012856).

REFERENCES

1. Sokmen, M.; Allen, D. W.; Akkas, F.; Kartal, N.; Acar, F. *Water Air Soil Pollut.* **2001**, *132*, 153.
2. Wu, C. H.; Yu, C. H. *J. Hazard. Mater.* **2009**, *169*, 1179.
3. Ghosh, T.; Cho, K. Y.; Ullah, K.; Nikam, V.; Park, C. Y.; Meng, Z. D.; Oh, W. C. *J. Ind. Eng. Chem.* **2013**, *19*, 797.
4. Gaya, U. I.; Abdullah, A. H. *J. Photochem. Photobiol. C: Photochem. Rev.* **2008**, *9*, 1.
5. Kuo, C. Y. *J. Hazard. Mater.* **2009**, *163*, 239.
6. Baojiang, J.; Chungui, T.; Wei, Zh.; Jianqiang, W.; Ying, X.; Qingjiang, P.; Zhiyu, R.; Youzhen, D.; Dan, F.; Jiale, H.; Honggang, F. *Chem.—Eur. J.* **2011**, *17*, 8379.
7. Lee, C.; Wei, X.; Kysar, J. W.; Hone, J. *Science* **2008**, *321*, 385.
8. Balandin, A. A.; Suchismita, Gh.; Wenzhong, B.; Irene, C.; Desalegne, T.; Feng, M.; Chun, N. L. *Nano Lett.* **2008**, *8*, 902.
9. Chen, J. H.; Jang, C.; Xiao, S.; Ishigami, M.; Fuhrer, M. S. *Nat. Nanotechnol.* **2008**, *3*, 206.

10. Fowle, J. D.; Allen, M. J.; Tung, V. C.; Yang, Y.; Kaner, R. B.; Weiller, B. H. *ACS Nano* **2009**, *3*, 301.
11. Liang, M.; Zhi, L. *J. Mater. Chem.* **2009**, *19*, 5871.
12. Adamson, D. H.; Schniepp, H. C.; Chen, X.; Ruoff, R. S.; Nguyen, S. T.; Aksay, I. A.; , Prud′Homme, R. K.; Brinson, L. C. *Nat. Nanotechnol.* **2008**, *3*, 327.
13. Yang, K.; Wan, J.; Zhang, S.; Zhang, Y.; Lee, S. T.; Liu, Z. *ACS Nano* **2011**, *5*, 516.
14. Iijima, S. *Nature* **1991**, *354*, 56.
15. Ebbesen, T. W.; Lezee, H. J.; Hiura, H.; Neentt, J. W.; Ghaemi, H. F.; Thio, T. *Nature* **1996**, *382*, 54.
16. Yu, Y.; Yu, J. C.; Chan, C. Y.; Che, Y. K.; Zhao, J. C.; Ding, L.; Ge, W. K.; Wong, P. K. *Appl. Catal. B* **2005**, *61*, 1.
17. Yu, Y.; Yu, J. C.; Chan, C. Y.; Che, Y. K.; Zhao, J. C.; Ding, L.; Ge, W. K.; Wong, P. K. *Appl. Catal. A* **2005**, *289*, 186.
18. Kim, Y. Y.; Yun, J.; Kim, H. I.; Lee, Y. S. *J. Ind. Eng. Chem.* **2012**, *18*, 392.
19. Wang, F.; Zhangc, K. *J. Mol. Catal. A: Chem.* **2011**, *345*, 101.
20. Linh, N. T. B.; Lee, K. H.; Lee, B. T. *J. Mater. Sci.* **2011**, *46*, 5615.
21. Bose, S.; Kuila, T.; Uddin, M. E.; Kim, N. H.; Lau, A. K.; Lee, J. H. *Polymer* **2010**, *51*, 5921.
22. Fang, Z.; Wang, K.; Wei, T.; Yan, J.; Song, L.; Shao, B. *Carbon* **2010**, *48*, 1686.
23. Stankovich, S.; Dikin, D. A.; Piner, R. D.; Kohlhaas, K. A.; Kleinhammes, A.; Jia, Y.; Wu, Y.; Nguyen, S. T.; Ruoff, R. S. *Carbon* **2007**, *45*, 1558.
24. Anjum, Q.; Sejal, S.; Pelagade, S.; Singh, N. L.; Mukherjee, S.; Tripathi, A.; Despande, U. P.; Shripathi, T. *J. Phys. Conf. Ser.* **2010**, *208*, 1.
25. Song, Z.; Hrbek, J.; Osgood, R. *Nano Lett.* **2005**, *5*, 1327.
26. Yun, J.; Kim, H. I.; Lee, Y. S. *J. Mater. Sci.* **2013**, *48*, 8320.
27. Moon, Y.; Jung, G.; Yun, J.; Kim, H. I. *Mater. Sci. Eng. B* **2013**, *173*, 1097.